SIMULATED PERFORMANCE OF THE WISCONSIN SUPERCONDUCTING ELECTRON GUN*

R. A. Bosch# and K. J. Kleman, Synchrotron Radiation Center, University of Wisconsin-Madison, 3731 Schneider Dr., Stoughton, WI 53589, USA
R. Legg, Jefferson Lab, 12000 Jefferson Avenue, Newport News, VA 23606, USA

Abstract

The Wisconsin superconducting electron gun is modeled with multiparticle tracking simulations using the ASTRA and GPT codes. To specify the construction of the emittance-compensation solenoid, we studied the dependence of the output bunch's emittance upon the solenoid's strength and field errors. We also evaluated the dependence of the output emittance upon the bunch's initial emittance and the size of the laser spot on the photocathode. The simulations indicate that a 200-pC bunch with peak current of 35 A and normalized emittance of about one mm-mrad can be produced for a free electron laser.

INTRODUCTION

A superconducting radiofrequency (SRF) electron gun has been designed to produce bunches that are suitable for a high-repetition-rate soft-xray free electron laser (FEL) [1–3]. The Department of Energy (DOE) is funding a 3-year project to build and test the electron gun for production of 200-pC bunches with normalized emittance of one mm-mrad at a repetition rate of 5 MHz.

The bunches will be created by laser illumination of a photocathode and then accelerated along the z-axis to energy of 4 MeV by a 200-MHz SRF cavity with peak field of 41 MV/m. Operation will commence with a Cu cathode, which can be replaced with a CsTe cathode for lower laser power. For a bunch created with $\sigma_x = \sigma_y = 1$ mm, initial normalized slice emittances ε_x and ε_y of ~1 mm-mrad and slice energy spread of ~0.5 eV are expected for these cathodes; the initial emittances are expected to be proportional to σ_x and σ_y [4, 5]. To minimize modulations in longitudinal phase space at the expense of slightly increased transverse emittance, "blowout" mode is employed, in which the initial bunch length is small compared to that of the accelerated bunch [6].

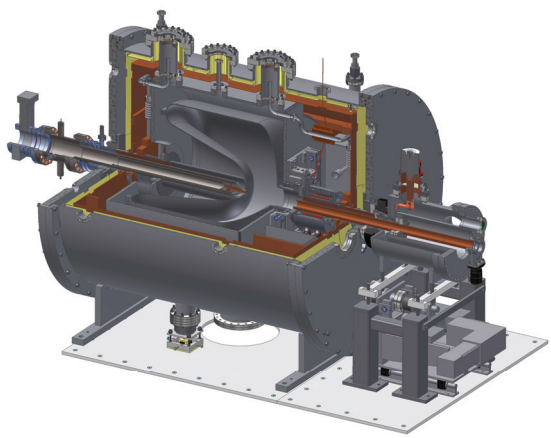

Figure 1: The photocathode, SRF cavity and HTS solenoid in the liquid-helium cryostat. Courtesy of M. Fisher.

The projected transverse emittance due to space charge is reduced by focusing in a high-temperature superconducting (HTS) solenoid [7], whose construction has been contracted to industry. In simulations, placing the solenoid immediately downstream of the SRF cavity gives the best performance. Figure 1 displays the photocathode, SRF cavity and HTS solenoid within the liquid-He-cooled cryostat.

For use in an FEL, the bunch may then be accelerated to energy of 85 MeV by a cryomodule containing eight TESLA 1.3-GHz SRF cavities, in which the bunch becomes longitudinally frozen and the emittance-compensation process is completed [8]. In simulations, we analyze the bunch at the exit of this cryomodule.

HTS SOLENOID

The solenoid specifications are based upon 100,000-particle simulations with the ASTRA code [9]. To model ideal performance, we performed 2D simulations in which the initial 200-pC bunch is a uniformly filled ellipsoid with zero transverse emittance, propagating along the z-

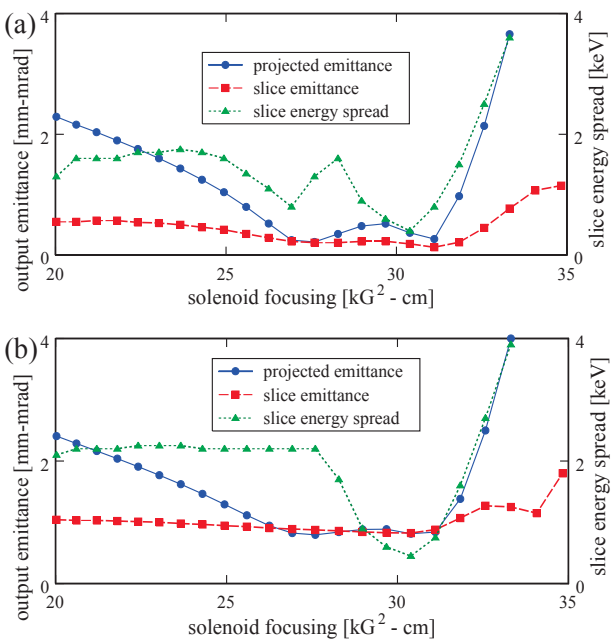

Figure 2: Normalized emittances and slice energy spread vs. solenoid focusing. (a) initial emittance is zero. (b) initial emittance is 0.8 mm-mrad.

*Work supported by DOE Award DE-SC0005264
bosch@src.wisc.edu

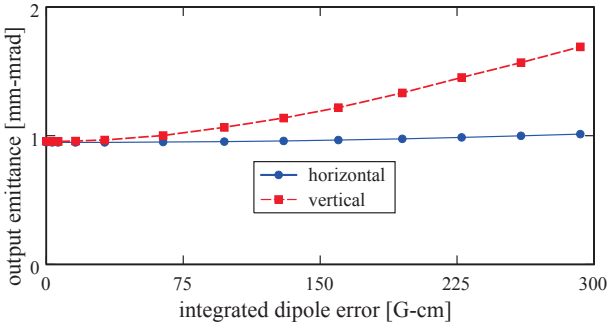

Figure 3: Projected horizontal and vertical normalized emittances vs. the solenoid's horizontal dipole error.

axis with $\sigma_x = \sigma_y = 0.8$ mm, $\sigma_t = 300$ fs, and initial kinetic energy of 0.5 eV.

Figure 2(a) shows the projected emittance versus the on-axis focusing strength $\int B_z^2 dz$ of a solenoid with physical length of 92.7 mm. The emittance and energy spread of a 500-particle slice in the longitudinal center of the bunch are also shown. The best performance is obtained with $\int B_z^2 dz = 31$ kG^2-cm, with output projected and slice emittances of 0.3 and 0.2 mm-mrad, slice energy spread of 0.5 keV and peak current of 33 A. Figure 2(b) models a Cu or CsTe cathode; the best performance is again obtained with a focusing strength of 31 kG^2-cm, which gives output projected and slice emittances of 0.8 mm-mrad and slice energy spread of 0.5 keV. Similar performance is obtained with solenoids of different lengths, provided that $\int B_z^2 dz = 31$ kG^2-cm.

ASTRA 3D simulations were used to obtain specifications for the solenoid's allowable field errors. In these 3D simulations with initial emittance of 0.8 mm-mrad for a Cu or CsTe photocathode, the output emittance is about 10% higher than in comparable 2D simulations.

Integrated dipole error on axis: $[(\int B_x dz)^2 + (\int B_y dz)^2]^{1/2} < 90$ G-cm. For a horizontal dipole-field error with the same longitudinal profile as the solenoidal field, this specification ensures that the projected vertical emittance increases less than 10%, while the increase in horizontal emittance is much smaller. The field error was modeled in ASTRA by a 3D field map for a 1-Hz dipole mode in an RF cavity. Figure 3 shows the horizontal and vertical emittances versus the integrated dipole error in 3D simulations. For a horizontal field error of 90 G-cm, the increases in projected horizontal and vertical emittances

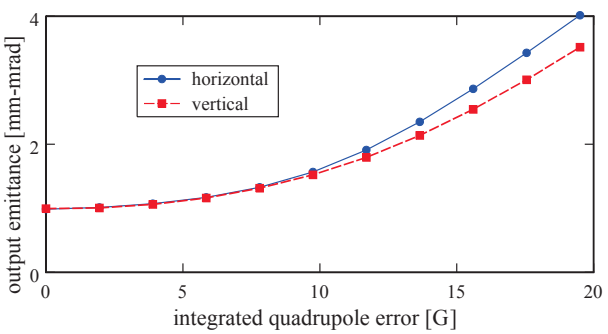

Figure 4: Projected horizontal and vertical normalized emittances vs. the solenoid's normal quadrupole error.

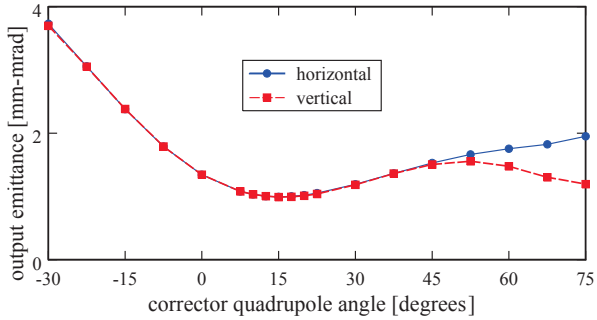

Figure 5: Projected horizontal and vertical normalized emittances vs. rotation angle of a quadrupole corrector, for a HTS solenoid with a 10-G quadrupole error.

can be reduced below 3% by a –0.8-mm horizontal offset of the solenoid. Correction of the trajectory angle at a distance of 0.6 m from the photocathode (where a corrector magnet is planned) requires a rotated dipole field with nearly the same integrated B field as the error.

Integrated quadrupole error on axis: $\{[\partial(\int B_x dz)/\partial x]^2 + [\partial(\int B_y dz)/\partial x]^2\}^{1/2} < 10$ G. For a quadrupole field error with the same longitudinal profile as the solenoidal field, this specification ensures that the projected emittance increases less than 10% when the error is compensated by a correction quadrupole whose rotation angle is within 7.5 degrees of its optimal value. Figure 4 shows the horizontal and vertical emittances for an uncorrected normal quadrupole field error. Figure 5 shows that a correction quadrupole located 0.6 m from the photocathode (with the same integrated quadrupole field as the error) keeps the emittance increase from a 10-G quadrupole error below 10% if the rotation is within 7.5° of optimal.

ASTRA VERSUS GPT

To confirm the ASTRA predictions and to study different initial bunch radii and emittances, we performed simulations using both the ASTRA and GPT codes [10]. We again analyzed the bunch properties after the emittance compensation is completed by acceleration to 85 MeV in a TESLA cryomodule. The codes were compared by performing 100,000-particle simulations for a realistic initial bunch that can be modeled by both codes: a bunch with truncated Gaussian radial and longitudinal profiles. To obtain approximately homogenous distributions, we use truncations at 0.8σ [11]. To model a laser illumination of 300 fs, we consider a longitudinal σ of 187.5 fs. Similar results were obtained for shorter illuminations, consistent with blowout mode.

For a Cu or CsTe photocathode with $\varepsilon_{x,y}$ [mm-mrad] ≈ $\sigma_{x,y}$ [mm], the lowest output emittance is obtained for a radial σ of 1.75 mm, in which case the initial σ_x and σ_y are 0.7 mm. For this radius, Fig. 6 shows the output emittances and energy spread vs. solenoid focusing for a bunch with zero initial emittance. The optimal focusing strength obtained by both GPT and ASTRA is 31 kG^2-cm.

Figure 7 shows the bunch properties vs. initial emittance for optimal solenoid focusing. For a Cu or

ISBN 978-3-95450-115-1

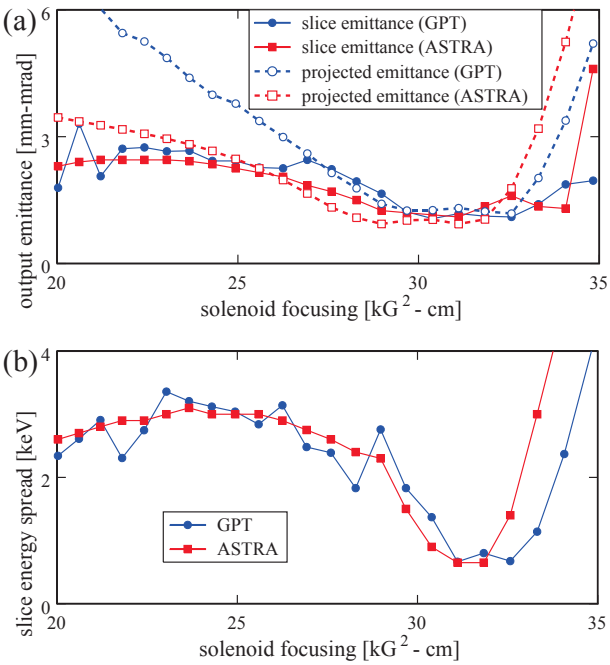

Figure 6: Bunch properties vs. solenoid focusing according to ASTRA and GPT, for an initial truncated Gaussian bunch distribution with σ_r of 1.75 mm and zero emittance. (a) projected and slice normalized emittances. (b) slice energy spread.

CsTe photocathode with initial transverse emittance of 0.7 mm-mrad, the projected bunch emittances and slice emittances are 1.3 mm-mrad, the slice energy spread is 0.5–1 keV, and the peak current is 35 A.

In our simulations of blowout mode, the output emittance of a 200-pC bunch from a Cu or CsTe photocathode illuminated by a truncated-Gaussian laser spot is ~50% higher than that of an initial ideal-ellipsoid bunch.

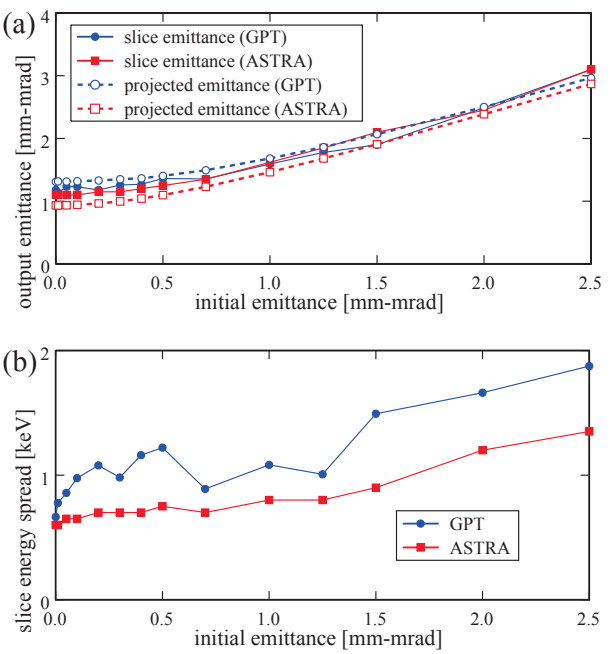

Figure 7: Bunch properties vs. initial emittance according to ASTRA and GPT, for an initial truncated Gaussian bunch distribution with σ_r of 1.75 mm. (a) projected and slice normalized emittances. (b) slice energy spread.

SUMMARY

For the Wisconsin superconducting electron gun, simulations have been performed with the ASTRA code in order to specify the strength and allowable error fields of the HTS solenoid. Additional simulations have demonstrated the approximate agreement between the ASTRA and GPT codes. For Cu or CsTe photocathodes, the electron gun can produce 200-pC bunches with peak current of 35 A, normalized projected and slice emittances of ~1 mm-mrad, and slice energy spread of 0.5–1 keV. These output bunches are suitable for a soft-xray FEL.

REFERENCES

[1] R. Legg, W. Graves, T. Grimm and P. Piot, in "Proceedings of the 11th European Particle Accelerator Conference, Genoa, Italy, 2008" (EPS-AG, Genoa, Italy, 2008), p. 469.

[2] R. Legg, in "Proceedings of the 24th Linear Accelerator Conference, Victoria, BC, Canada, 2008" (TRIUMF, Vancouver, BC, Canada, 2009), p. 658.

[3] R. Legg, M. Allen, M. Fisher, Z. Hjortland, K. Kleman, T. Grimm and M. Pruitt, in "Proceedings of the 45th ICFA Advanced Beam Dynamics Workshop on Energy Recovery Linacs, Ithaca, NY, 2009" (Cornell, Ithaca, NY, 2010), p. 45.

[4] W. S. Graves, L. F. DiMauro, R. Heese, E. D. Johnson, J. Rose, J. Rudati, T. Shaftan and B. Sheey, in "Proceedings of the 2001 Particle Accelerator Conference, Chicago" (IEEE, Piscataway, NJ, 2001), p. 2227.

[5] V. Miltchev, Ph.D. thesis, Humbolt University, Berlin, 2006.

[6] O. J. Luiten, S. B. van der Geer, M. J. de Loos, F. G. Kiewiet and M. J. van der Wiel, Phys. Rev. Lett. 93, 094802 (2004).

[7] R. Gupta, M. Anerella, I. Ben-Zvi, G. Ganetis, D. Kayran, G. McIntyre, J. Muratore, S. Plate, W. Sampson, M. Cole and D. Holmes, in "Proceedings of the 2011 Particle Accelerator Conference, New York" (PAC'11 OC / IEEE, NY, 2011), p. 1127.

[8] L. Serafini and J. B. Rosenzweig, Phys. Rev. E 55, 7565 (1997).

[9] G. Pöplau, U. van Rienen and K. Flöttmann, in "Proceedings of the 10th European Particle Accelerator Conference, Edinburgh, 2006" (EPS-AG, Edinburgh, 2006), p. 2203.

[10] M.J. de Loos and S.B. van der Geer, in "Proceedings of the 5th European Particle Accelerator Conference, Sitges, Spain, 1996" (EPS-AG, Sitges, 1996), p. 1241.

[11] P. Musumeci, J. T. Moody, R. J. England, J. B. Rosenzweig and T. Tran, Phys. Rev. Lett. 100, 244801 (2008).